A NOVEL ZERO CURRENT SWITCHING HIGH FREQUENCY INVERTER FOR INDUCTION HEATING

Shimajiri Satoru
Tokyo University of Mercantile Marine
2-1-6 Etchujima, Koto-ku, Tokyo 135-8533, JAPAN
Phone 81-3-5245-7412, Fax 81-3-5245-7336

Hatanaka Yoshihiro
Tokyo University of Mercantile Marine
2-1-6 Etchujima, Koto-ku, Tokyo 135-8533, JAPAN
Phone 81-3-5245-7412, Fax 81-3-5245-7336

ABSTRACT - In this paper, a novel zero current switching (ZCS) high frequency inverter for induction heating is proposed. The ZCS characteristics are investigated from both the numerical analysis and the experiment

1.INTRODUCTION

Recently, many types of high-frequency inverters have been developed for induction heating applications. For the high frequency power supply, soft-switching techniques such as Zero Current Switching (ZCS) and zero voltage switching (ZVS) have been proposed to suppress the switching loss and surge voltage[1]-[6].

Generally, insulated gate bipolar transistor (IGBT) is extensively used for switching devices in the high-frequency and high-power applications. However, a problem of a tail current, which occurs in the forced turn-off of the switching current of IGBT, is inherent in the power supply using IGBT. Thus, the ZCS operation is desirable to reduce the switching loss caused from the tail current in these applications

In this paper, the novel zero current switching high-frequency inverter (N-ZCS HF-INV) is proposed as an improved type of conventional single ended push pull inverter (SEPP INV). The ZCS characteristics on the basis of numerical analysis are studied and experimented.

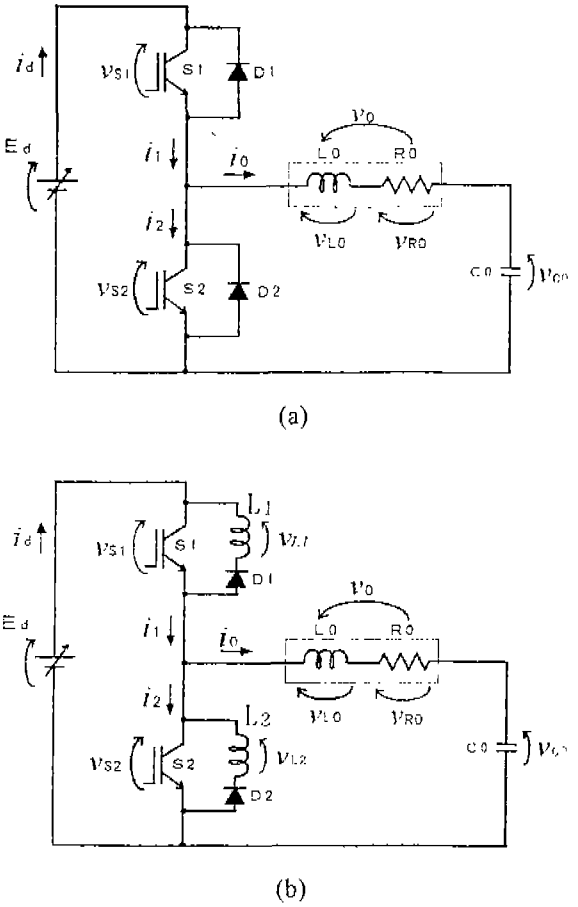

Figure 1 (a) Conventional single ended push pull inverter (b) Novel ZCS high frequency inverter

2.PROPOSED ZCS HIGH FREQUENCY INVERTER

Figure 1(a) shows the configuration of conventional SEPP INV. The remarkable feature of the proposed N-ZCS HF-INV as shown in figure 1(b) is reactor of L_1,L_2 connected in series with the anti-parallel diodes of the conventional SEPP INV. In the conventional SEPP INV, a short circuit condition may be occurred in the case of operating frequency is smaller than resonant frequency because of the reverse recovery current of the diode D_1 or D_2 as shown in figure 2 (a).

However, the N-ZCS HF-INV proposed in this paper

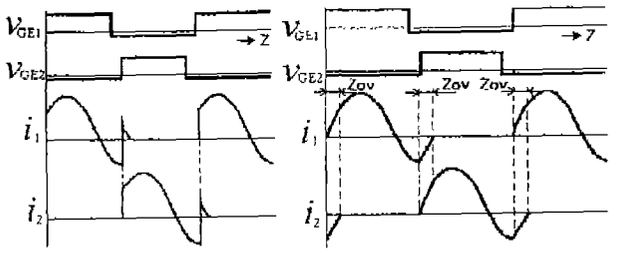

(a) (b)

Figure 2 Switching waveforms
(a)SEPP INV. (b) N-ZCS HF INV.

is enable to operate under ZCS condition based on the overlapping commutation phenomenon, which occurs in the case when S_1 turns on during D_2 conducts or S_2 turns on during D_1 conducts due to connection of reactor of L_1,L_2.

At the switching operation in the steady-state, there is no problem of switching loss caused by the tail current because the IGBTs for main switch turns off after the switch current changes its direction and flows through the anti-parallel diode. Moreover, the switches turn-on at low di/dt suppressed switching losses. In figure 1, The series RL circuit enclosed with the dotted line represents an equivalent circuit of load for induction heating using a surplus energy at nighttime in a capacity to generate electric power in Japan.

3.CIRCUIT OPERATION

Switching modes of N-ZCS HF inverter are classified into seven modes due to switching condition. these switching modes are as follows:

Mode a : S_1 single conduction mode
Mode b . D_1 single conduction mode
Mode c : S_2,D_1 double conduction mode
Mode d : S_2 single conduction mode
Mode e : D_2 single conduction mode
Mode f : S_1,D_2 double conduction mode
Mode g : off mode (All the switching devices are off state mode.)

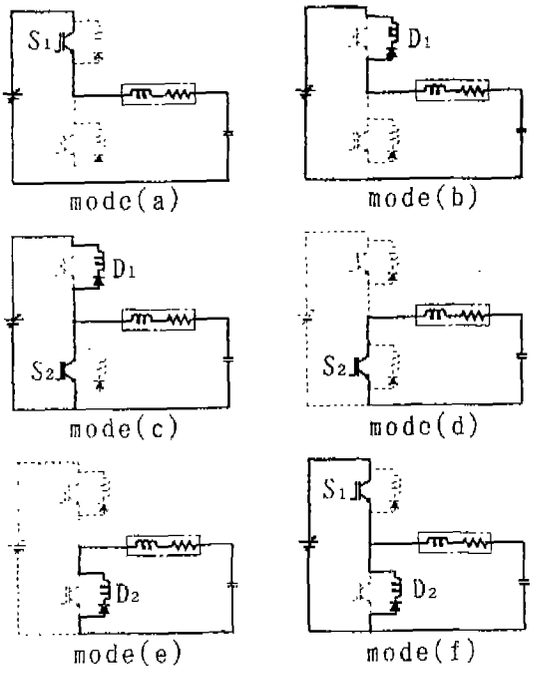

Figure 3 Switching modes

Fig.3 shows principles of switching operation. At normalized time z=0(refer to table 1) during the diode D_2 conducting, when the switch S_1 is turned on by the gate-emitter voltage v_{GE1}, then the diode current i_2 of D_2 lineally decreases to zero due to the reactor L_2 simultaneously. The switch current $i_1$of S_1 is

$$i_1 = i_2 + i_O \tag{1}$$

where i_2 is the reactor current of L_2, i_O is the reactor current of L_O in the switching. Because the switch current i_1 of S_1 can be replace with the reactor current, which is a continuous value, it is gradually increase from zero. Hence, this time interval of z_{OV} is S_1, D_2 double conduction mode that is the overlapping commutation time. From when the diode current i_2 turns zero, the switch S_1 singly conducts. When resonant current i_1 reaches zero and then i_1 is negative, thc anti-parallel diode D_1 starts to conduct. Like S_1, D_2double conduction mode, during the diode D_1 conducting, if S_2 is triggered, S_2 also starts conducting. From when the diode current i_1 turns zero, the switch S_2 singly conducts. When resonant current i_2 reaches zero and then i_2 is negative, the anti-parallel diode D_2 starts to conduct.

In this periodical switching operation, all switching

devices accomplish ZCS operation.

For circuit analysis, some normalized parameters are introduced and defined as indicated in Table 1. State variables in the numerical analysis are

$$X(t) = [i_O \quad i_1 \quad i_2 \quad v_{CO}]^T \tag{2}$$

where i_1, i_2 and i_O are each inductance currents, v_{CO} is capacitance voltage.

Normalized values are

$$X(z)=[i_O^* \quad i_1^* \quad i_2^* \quad v_{CO}^*]^T \tag{3}$$

where i_1^*, i_2^*, and i_O^* are normalized currents, v_{CO}^* is normalized voltage

The normalized state equations in each switching mode are as follows:

Mode a : dX/dz=A1X+B1 (4)
Mode b : dX/dz=A2X+B2 (5)
Mode c : dX/dz=A3X+B3 (6)
Mode d : dX/dz=A4X+B4 (7)
Mode e : dX/dz=A5X+B5 (8)
Mode f : dX/dz=A6X+B6 (9)

where

$$A1 = A6 = \begin{bmatrix} -\frac{2\pi\lambda}{\mu} & 0 & 0 & -\frac{2\pi}{\mu} \\ -\frac{2\pi\lambda}{\mu} & 0 & 0 & -\frac{2\pi}{\mu} \\ 0 & 0 & 0 & 0 \\ \frac{2\pi}{\mu} & 0 & 0 & 0 \end{bmatrix}$$

$$A2 = \begin{bmatrix} -\frac{2\pi\lambda}{\mu(\alpha+1)} & 0 & 0 & -\frac{2\pi}{\mu(\alpha+1)} \\ -\frac{2\pi\lambda}{\mu(\alpha+1)} & 0 & 0 & -\frac{2\pi}{\mu(\alpha+1)} \\ 0 & 0 & 0 & 0 \\ \frac{2\pi}{\mu} & 0 & 0 & 0 \end{bmatrix}$$

$$A3 = A4 = \begin{bmatrix} -\frac{2\pi\lambda}{\mu} & 0 & 0 & -\frac{2\pi}{\mu} \\ 0 & 0 & 0 & 0 \\ \frac{2\pi\lambda}{\mu} & 0 & 0 & \frac{2\pi}{\mu} \\ \frac{2\pi}{\mu} & 0 & 0 & 0 \end{bmatrix}$$

Table 1 Normalized parameters

[Standard Value]	
Inductance	L=Lo
Capacitance	C=Co
Resistance	R=Ro
Impedance	$Z=\sqrt{L/C}$
Voltage	E=Ed
Current	I=E/Z
Power	P=E·I
[Normalized Parameters]	
Reactor ratio	α =L1/L=L2/L
Resistance	$\lambda=R\sqrt{L/C}$
Frequency	$\mu = 2\pi fo\sqrt{LC}$
Time	T=1/fo fo:output frequency
[State Variables]	
Voltage	v(z)*=v(t)/E
Current	i(x)*=i(t)/I
Time	z=fo·t =t/T

$$A5 = \begin{bmatrix} -\frac{2\pi\lambda}{\mu(\alpha+1)} & 0 & 0 & -\frac{2\pi}{\mu(\alpha+1)} \\ 0 & 0 & 0 & -\frac{2\pi}{\mu} \\ \frac{2\pi\lambda}{\mu(\alpha+1)} & 0 & 0 & \frac{2\pi}{\mu(\alpha+1)} \\ \frac{2\pi}{\mu} & 0 & 0 & 0 \end{bmatrix}$$

$$B1 = \frac{2\pi}{\mu}[1 \quad 1 \quad 0 \quad 0]^T$$

$$B2 = \frac{2\pi}{\mu(\alpha+1)}[1 \quad 1 \quad 0 \quad 0]^T$$

$$B1 = \frac{2\pi}{\mu\alpha}[0 \quad 1 \quad 1 \quad 0]^T$$

$$B4 = 0$$

$$B5 = 0$$

$$B6 = \frac{2\pi}{\mu}\left[1 \quad \frac{\alpha+1}{\alpha} \quad \frac{1}{\alpha} \quad 0\right]^T$$

4.EFFECT OF REACTOR RATIO

A special feature for the proposed inverter is reactor of L_1 and L_2 connected with the anti-parallel diodes. The overlapping commutation phenomenon and ZCS characteristics are depend on these reactor value. Figure 4 illustrates the switching waveforms in some reactor ratio of $\alpha = L_1/L_O$. The current waveform shown as figure 4(b) is accomplished by the switching operation at

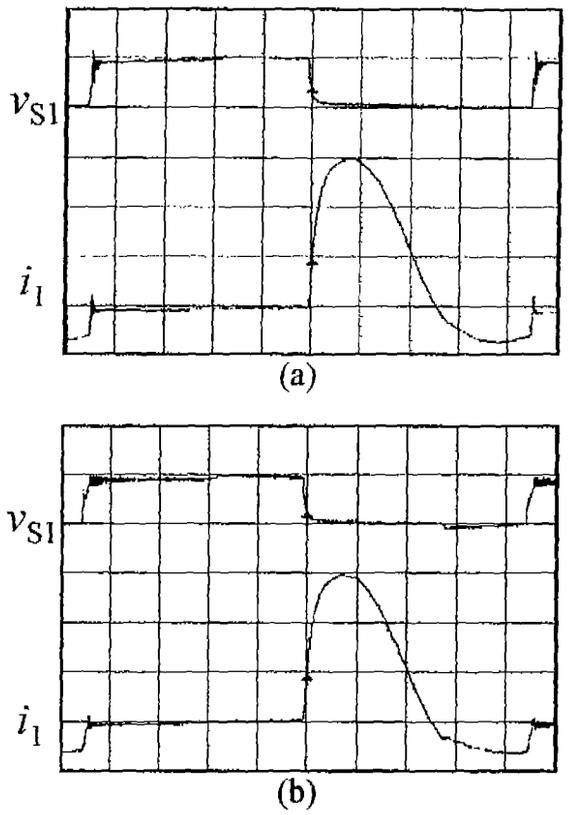

Figure 4 ZCS waveforms with some reactor ratio of α (a) α =0.1 (b) α =0.5
(100V/div,0.5A/div,20 μ s/div)

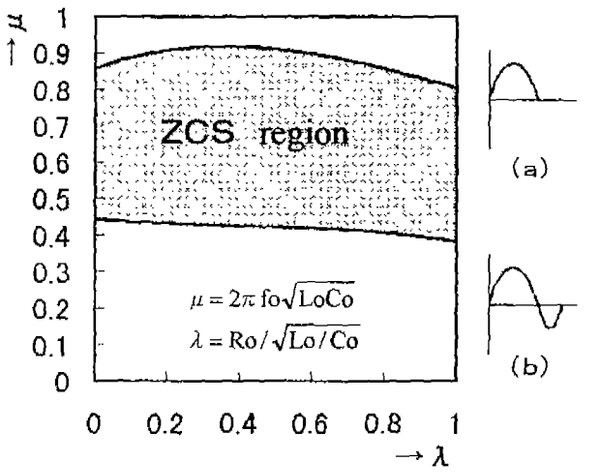

Figure 5 ZCS operation region
(a)A current waveform on upper boundary line in ZCS region (b) A current waveform on bottom boundary line in ZCS region

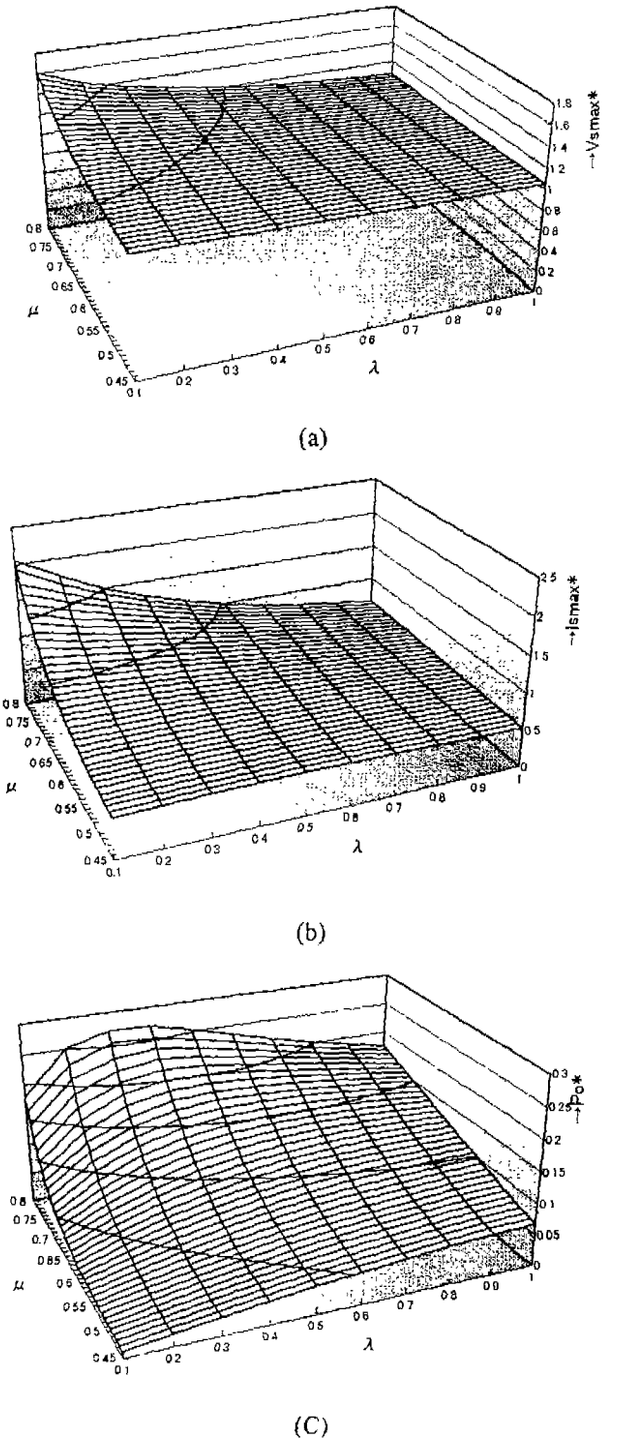

Figure 6 A three-dimensional distribution of each characteristic value as functions of μ and λ in ZCS region (a)Distribution of Vsmax* (b) Distribution of Ismax* (c) distribution of Po*

low di/dt in comparison with the waveform shown as figure 4(a). Therefore diode reverse recovery current and voltage spikes caused by the parasitic inductance are reduced.

In this paper, the ZCS characteristics in α=0.5 because a maximum voltage of switch and the conduction loss of each reactors increase with an increase in reactor ratio of α.

5.ZCS OPERATION REGION

For ZCS operation, it is necessary to grasp the ZCS region where ZCS operation is also guaranteed in case of variable load (normalized resistance λ) or variable frequency (normalized frequency μ), as taking measures to meet voltage spikes and surge currents. Figure 5 illustrates the ZCS region on the basis of numerical analysis in the normalized μ and λ plane. In this region, the soft switching of all switches can be accomplished by the ZCS operation. The ZCS operation can be achieved without the reactor L_1 and L_2 only in the case of the switches turn off at the time when the switch current of S_1,S_2 or the diode current of D_1,D_2 turns to zero; these current waveforms are referred to figure 5(a),(b). However, for the N-ZCS HF-INV, the parameters of μ and λ should be designed within the dotted area to ensure the soft switching.

For resonant inverter, a normalized maximum voltage of switch (Vsmax*) and the normalized maximum current of switch (Ismax*) such as the switching stress generally tend to increase, it is necessary to grasp the relationship between these specific values and a normalized output power (Po*).

A three-dimensional distribution of each characteristic value in the ZCS region is depicted in figure 6. In the majority of the ZCS region, Vsmax* can be suppressed to 1.4times or less of the power supply voltage. However, Vsmax* become higher with an increase in μ and a decrease in λ. Thus, to reduce the switching stress, it is necessary to avoid to operate in such a parameters. Like Vsmax*, Ismax* becomes also higher with increase of μ and decrease of λ. The normalized power of the load, Po*, tends to increase, when the value of λ is in the range of 0.2 to 0.6. The N-ZCS HF-INV for induction heating is designed and operated by using λ=0.6, μ=0 7 in consideration of result of these analysis.

Table 2 Design specification

Parameters
Lo=99μH, L1=L2=50μH, μ=0.75, λ=0.7,
Co=1.03μF, Ro=6.25Ω, α=0.5
Ed=172V, fo=15.2kHz, Po=1kW

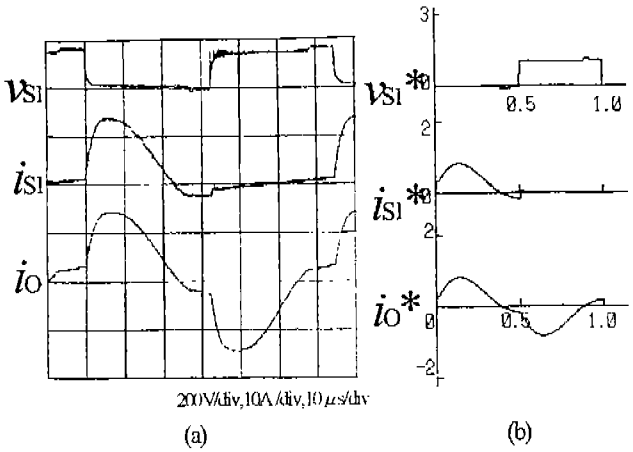

Figure 7 Switching waveforms of N-ZCS HF INV. (a)experimental waveforms (b)theoretical waveforms

6.EXPRIMENTAL RESULTS

In this experiment, the N-ZCS HF INV is designed for output power Po=1kW at operating frequency of approximately 18kHz. Table 2 indicates the design specification of the N-ZCS HF-INV. Figure 7 illustrates theoretical waveforms on the basis of numerical analysis. The tendency of output waveforms shows good agreement respectively. Hence, the results of numerical analysis are verified experimentally.

ZCS operation utilizing overlapping commutation phenomenon based on consideration of reactor ratio of α is obtained for all switching devices, and the stable operation due to reduction in reverse recovery current and voltage spikes is achieved. Figure 8 shows the efficiency measurement of the N-ZCS HF INV as a function of the

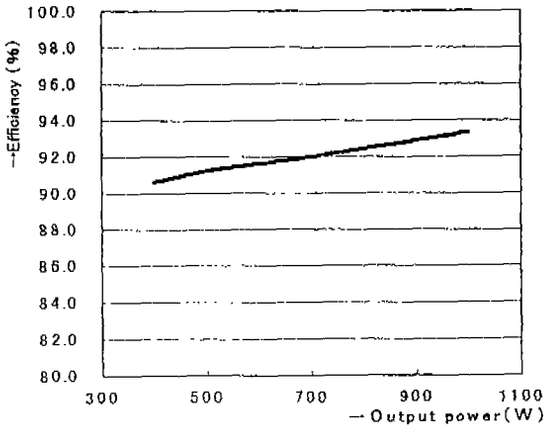

Figure 8 Experimental efficiency(=output power/input power) as functions of output power

output power. Due to the ZCS operation utilizing the overlapping commutation phenomenon, the experimental efficiency reaches approximately 93%.

7.CONCLUSION

In this paper, the N-ZCS HF INV utilized the overlapping commutation phenomenon is proposed. As a result of numerical analysis based on consideration of reactor ratio of α, the distribution of each characteristic value in the ZCS region is clarified.

Experimental results on the basis of numerical analysis show that the stable ZCS operation suppress the reverse recovery current and spike voltage.

For N-ZCS HF INV, there is no problem of tail current losses because IGBTs sinusoidal turn off ; ZCS operation reduce the switching losses. Therefore, high efficiency is achieved.

As for proposed N-ZCS HF INV, it is expected for not only the power supply for induction heating but also the application as high-frequency link converter.

8.REFERENCE

[1] S. Kubota, Y. Hatanaka, "A Novel High Frequency Power Supply for Induction Heating", proceedings of PESC'98 Vol.1 pp.165-171, 1998

[2] S.Shimajiri, Y.Hatanaka, "Novel Two-Transistor Type ZCS High Frequency Inverter for Induction Heating", proceedings of National Convention of I.E.E.Japan, p.4.239

[3]Y.Hatanaka, M.Yamagami, H. Okada , "High Frequency Power Supply for Ultrasonic Homogenizer Enabling Great Reduction of NOx", Journal of the M.E.S.J., Vol,29 No.11, pp.788-797(1994-11)

[4]Y. Hatanaka, et al., "Applications of Soft Switching High Frequency Inverter for Reduction of NOx and Particulates", proceedings of ISME Yokohama'95 Vol.1(1995-7)

[5]M.K.Kazimierczuk, S.Wang, "Frequency-Domain Analysis of Series Resonant Converter for Continuous Conduction Mode", IEEE Trans. Power Electron., Vol.7, No.2, pp.270-279, April 1992.

[6]Y.Hatanaka, S.Kubota, Y.Sekiya , "Novel Zero Current Switching High Frequency Inverter Applied for an Emission Control in Diesel Engine", proceedings of EPE97', Vol.4, pp.315-320, Sep. 1997.